

Effects of Freezing on Intratumoral Drug Transport

Bumsoo Han and Ka Yaw Teo

Abstract— Efficacy of many novel therapeutic agents are impaired by hindered interstitial diffusion in tumor. In the context of overcoming this drug delivery barrier, a hypothesis was postulated that freeze/thaw (F/T) may induce favorable changes of tumor tissue microstructure to facilitate the interstitial diffusion. This hypothesis may also be relevant to develop a mechanistically derived chemotherapeutic strategy for cryo-treated tumors. In the present study, this hypothesis was tested by characterizing the effects of F/T on the interstitial diffusion using an *in vitro* engineered tumor model (ET). The diffusion coefficients of FITC-labeled dextran was measured within the frozen/thawed and unfrozen ETs. The results showed that the diffusion coefficients increased after F/T but the extent of increase was dependent on the size of dextran. This implies that the combination of cryosurgery and chemotherapy should be designed considering the biophysical changes of tissues after freeze/thaw and the diffusion characteristics of drug molecules.

I. INTRODUCTION

TRANSPORT in tumor interstitium is one of the most difficult steps in both systemic and local administration of therapeutic agents. Although many novel therapeutic agents have been developed for decades, the efficacy of these agents are impaired due to limited transport in tumor interstitium. This limited interstitial transport is contributed by higher interstitial fluid pressure (IFP) and denser collagen extracellular matrix (ECM) structure of tumors than normal tissues [1]. For successful interstitial drug transport, therefore, these physiological barriers should be overcome. A wide variety of methods have been proposed and investigated to enhance the interstitial transport, but the main strategies are either lowering tumor IFP [2], or modulating tumor ECM structure [3]. However, due to complex interaction of various physiological parameters, the control or manipulation of tumor IFP and ECM structure still warrant further research. Moreover, if possible, methods to facilitate both barriers are desirable to enhance both convection and diffusion processes in tumor interstitium.

In the context of overcoming these adverse transport barriers, a hypothesis is postulated that freezing-induced

biophysical changes may enhance the interstitial drug transport. The rationale of this hypothesis based on recent studies [4, 5] reporting that the ECM microstructure of tissue is loosened after freezing, and the extent of this alteration is associated with freezing conditions. Thus, the alteration of the ECM microstructure may be able to increase the diffusion coefficient and hydraulic conductivity of tumor interstitium so that the interstitial drug transport can be enhanced. Since localized freezing (i.e., cryosurgery) has already been employed to treat small tumors, compared to other strategies to overcome the drug transport barriers, the use of cryosurgery as an adjuvant therapy to chemotherapy may clinically be feasible and more easily adaptable.

The proposed hypothesis has another important aspect of designing mechanistically derived chemotherapy for cryo-treated tumors. Synergistic effects of various chemotherapeutic agents with cryo-treatment have been reported [6-8], but the underlying interaction mechanisms are poorly understood. Thus, no clinical guideline has been established to determine the type, dosage, and administration timing of chemotherapeutic agents for the maximized efficacy [9].

In the present study, the hypothesis was tested by characterizing the effects of F/T on the interstitial diffusion using an *in vitro* engineered tumor model (ET) of breast cancer. The diffusion coefficients of FITC-labeled dextran in the frozen/thawed and unfrozen ETs were measured using an integrative optical imaging method [10, 11]. The relevance of the F/T-induced changes to intratumoral drug transport was discussed.

II. MATERIALS AND METHODS

A. Cells Culture and Engineered Tumor Model

A human breast cancer cell line (MCF-7) was maintained in culture medium (D-MEM/F12, Life Technologies) supplemented with 5% fetal bovine serum, 1% penicillin/streptomycin and 0.01mg/ml of insulin. Cells were incubated in 75cm² T-flasks at 37°C and 5% CO₂ environment. When cells were 60 ~ 80% confluent, they were collected on a regular basis.

To construct 2mL of engineered tumor model (ET), a pellet of MCF-7 was re-suspended in collagen solution. The detailed preparation protocol of ET was described in [4]. Briefly speaking, MCF-7 cells were mixed with type I

Manuscript received April 7, 2009. This work was supported in part by the National Science Foundation (CBET-0747631), and National Institute of Bioengineering and Biomedical Imaging (R01 EB008388).

Bumsoo Han is with the University of Texas at Arlington, Arlington, TX 76019 USA (corresponding author, phone: 817-272-1123; fax: 817-272-5010; e-mail: bhan@uta.edu).

Ka Yaw Teo is with the University of Texas at Arlington, Arlington, TX 76019 USA (e-mail: ka.teo@mavs.uta.edu).

collagen (Collagen I High Protein Rat Tail, BD Science) and the other reagents so that the final collagen concentration and cell concentration was 3mg/mL and 200,000 cells/mL respectively. Then, the mixture was placed in a one-well chamber slide (Nunc Lab-Tek II Chamber Slide, Fisher Scientific) and incubated for 1 hour at 37°C and 5% CO₂ environment for polymerization. After polymerization, 2 mL of complete cell culture medium was added to avoid dehydration and it was incubated for 24 hours until the experiment.

B. Freeze/Thaw Protocol

The ETs were frozen on a directional solidification stage [12] from 4 °C to -20 °C at the rate of 5 °C/min. The directional solidification stage consisted of two constant temperature reservoirs, which are at different temperatures and separated by an adjustable gap. The first reservoir was held at 4.0 ± 0.2 °C and the temperature of the other reservoir was set at -20.0 ± 0.2 °C. The chamber slide was moved from the high temperature reservoir to the low temperature one over the gap at a precisely controlled velocity. Half of each gel was frozen, leaving a frozen and unfrozen section of the same sample. The samples were passively thawed at room temperature after freezing.

C. Integrative Optical Imaging (IOI)

After F/T, the diffusion coefficients of both frozen/thawed and unfrozen region of the ETs were measured using an integrative optical imaging (IOI) method. The detailed description of the IOI method is available in [10, 11]. Briefly speaking, a small amount (25 - 50 pL) of a fluorescent probe with known size was injected into the ET sample using a microinjection system (MINJ-D-BDCI, Tritech) as shown in Fig. 1.

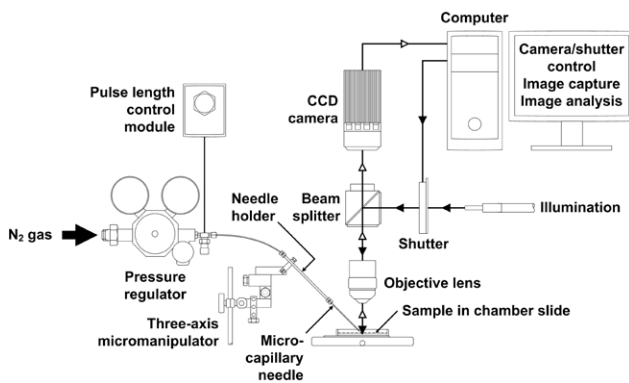


Fig. 1. Schematic diagram of the IOI experimental setup. FITC-labeled dextran was injected to ETs through micro-capillary needles. After the injection, the diffusion of dextran was imaged with a CCD camera at 1 second interval.

For the present study, four different sizes of FITC-labeled dextran were used - whose molecular weights are 4 kDa (hydrodynamic radius = 1.3 nm), 40 kDa (5.1 nm), 70 kDa (6.3 nm) and 500 kDa (12.6 nm) [13]. After the injection,

the diffusion of the fluorescent probe will be imaged at 1 second time interval. Then, the fluorescence intensity of the images will be quantified using image processing software (MATLAB, Mathworks). The intensity profiles were curve-fitted to the analytic solution of diffusion from a point source to obtain an estimated value of diffusion coefficient as below.

$$I(r, \gamma_i) = E_i(\gamma_i) \exp\left[-(r/\gamma_i)^2\right] \quad (1)$$

where E_i is an amplitude term compensating the de-focused point spread function, and the term γ_i is given by

$$\gamma_i^2 = 4D(t_i + t_o) \quad (2)$$

The measured intensity profile at each time step was curve-fitted for γ_i and subsequently the diffusion coefficient, D , was determined by (2). In order to compensate the finite size of the injection, a virtual time, t_o , was added while evaluating the diffusion coefficient D . The diffusion coefficients were measured with at least three ETs ($n \geq 3$) for all cases.

III. RESULTS AND DISCUSSION

Brightfield micrograph of a typical engineered tumor model of MCF-7 breast cancer cells are shown in Fig. 2. The cells are uniformly distributed throughout the collagen matrix and grow in 3D environment simulating tumor tissue structure. Although the cell density is lower and the porosity of ECM is higher than tumor tissues, this model contains important tissue-like features including cell-cell interaction and cell-ECM interaction while providing the feasibility of control and manipulation.

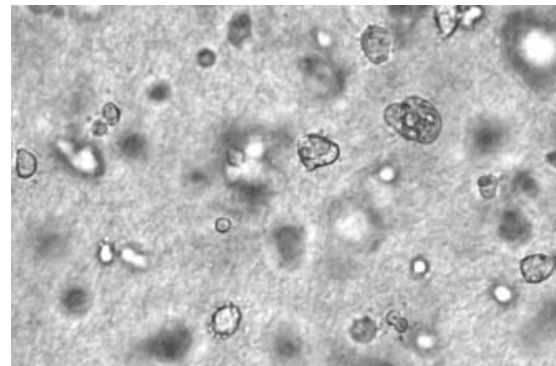


Fig. 2. Micrograph of a typical engineered tumor model of MCF-7 human breast cancer cells. The cells are distributed in 3-D environment simulating tumor tissue structure.

Sequential fluorescence micrographs are presented in Fig. 3 showing a typical diffusion of 40kDa dextran in the frozen/thawed and unfrozen ETs. Immediately after the injection (i.e., $t = 0$ s), dextran distributes comparably in both frozen and unfrozen ETs. However, at the later time points, dextran in the frozen ET shows more rapid diffusion

than dextran in the unfrozen ET.

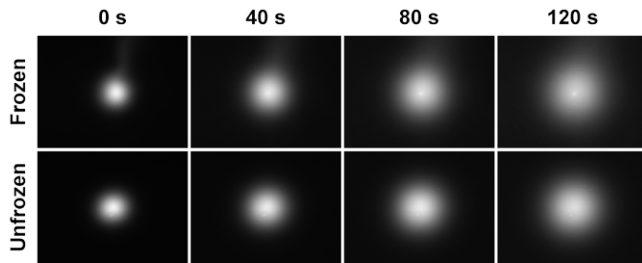
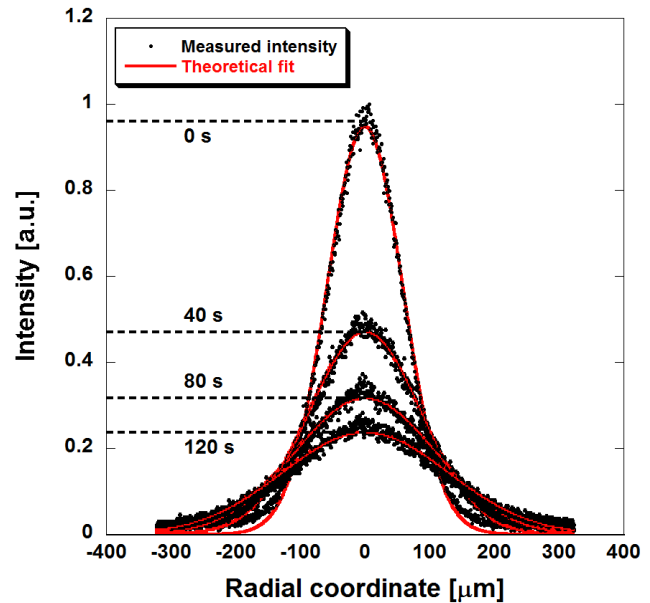


Fig. 3. Fluorescence micrographs of a typical diffusion of 40kDa dextran in the frozen and unfrozen ETs. Dextran diffuses faster in the frozen ETs.

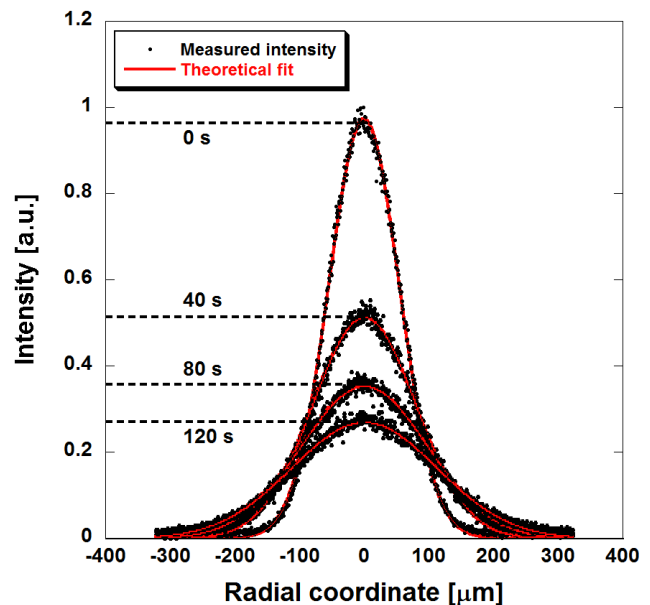
The corresponding fluorescence intensity profiles are shown in Fig. 4 for quantitative comparison. The measured intensity profiles, noted with dots, were normalized to the maximum intensity at $t = 0$ s, and curve-fitted to the analytic solution of diffusion from a point source as shown in (1). Generally, all the profiles are well fitted to the analytic solution. The maximum intensity of the frozen/thawed ET decays more rapidly than that of the unfrozen ET. In the frozen/thawed ET, the maximum intensity decreases from 1 to 0.24 during 120 seconds. During the same time period, the maximum intensity of the unfrozen ET decays to 0.27. The faster decay of the intensity infers that more rapid diffusion of FITC-labeled dextran in the radial direction. This may be caused by enlarged pore structure after F/T. Several recent studies reported that F/T induced the microstructural changes of the extracellular matrix of tissue including enlarged pores [4, 5], which could lead the enhancement of the interstitial diffusion after F/T.

The diffusion coefficients of all dextrans within either frozen/thawed or unfrozen ETs are summarized in Fig. 5 ($n \geq 3$ for all measurements). For 4kDa dextran, there is no noticeable difference in diffusion coefficients ($P = 0.4$). In the contrary, the diffusion coefficients of dextrans of bigger sizes increase in the frozen ETs ($P < 0.05$). However, the extent of the increase depends on the size of dextran molecules: from $4.90 \times 10^{-11} \text{ m}^2/\text{s}$ to $5.45 \times 10^{-11} \text{ m}^2/\text{s}$ for 40kDa (11.2 % increase), from $4.15 \times 10^{-11} \text{ m}^2/\text{s}$ to $4.56 \times 10^{-11} \text{ m}^2/\text{s}$ for 70kDa (9.8 % increase), and from $1.69 \times 10^{-11} \text{ m}^2/\text{s}$ to $1.94 \times 10^{-11} \text{ m}^2/\text{s}$ for 500kDa (14.8 % increase). This trend may be explained by considering the extent of F/T-induced ECM structural changes and the size of dextran molecules. For the smallest dextran (4kDa), the molecules are so small that its diffusion might not be significantly hindered by the collagen ECM prior to F/T. Thus, the enlarged pore structure of ECM by F/T may not affect its diffusion substantially. However, as the size of dextran increases, the effects of the enlarged pores become apparent. This implies that their diffusion has been hindered by the collagen ECM structure prior to F/T and

the hindrance is lessened due to the F/T-induced enlarged ECM pores.



(a)



(b)

Fig. 4. Intensity profiles of 40kDa dextran in frozen and unfrozen ETs. (a) Diffusion in the frozen ET. (b) Diffusion in the unfrozen ET. Dextran diffuses more rapidly in the frozen ETs.

This result could be relevant to enhancing intratumoral drug transport. If the tumor ECM structure, which has been reported as very dense collagen microstructure with low diffusion coefficients, is altered by F/T-induced cell-fluid-matrix interaction, this could be beneficial to the interstitial transport of drugs and therapeutic agents. However, the magnitude of enhancement might depend on the relative

size of drug molecules and enlarged pores.

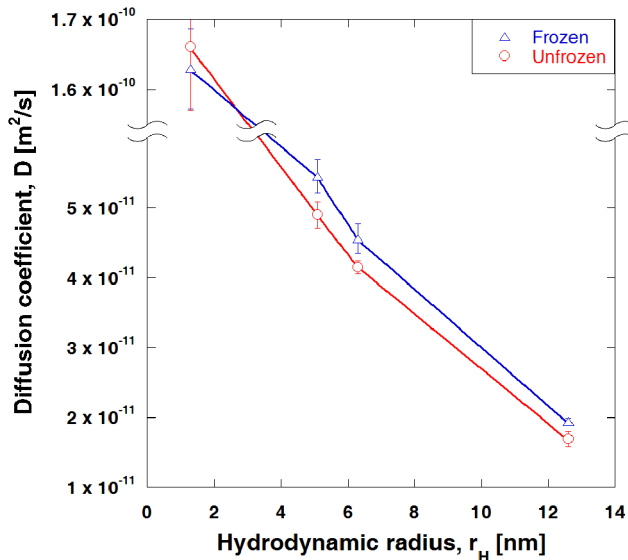


Fig. 5. Diffusion coefficients of FITC-labeled dextran in frozen and unfrozen ETs. Diffusion coefficients generally increase after F/T, but the magnitude of increase depends on the size of dextran.

IV. CONCLUSION

Effects of freezing on interstitial drug transport were investigated by measuring diffusion coefficients of several sizes of dextran molecules. The results showed that the diffusion coefficients increase after F/T but the extent depends on the size of dextran. Thus, when chemotherapy is planned after cryosurgery, the size of drug molecules and F/T-induced structural changes seem to be important parameters to be considered. Further research is warranted to quantify the effects of F/T conditions such as cooling rates and freezing temperatures on the ECM microstructure and the diffusion coefficients. In addition, the changes of hydraulic conductivity also need to be quantified.

REFERENCES

- [1] R. K. Jain, "Transport of molecules, particles, and cells in solid tumors," *Annu. Rev. Biomed. Eng.*, vol. 01, pp. 241-263, 1999.
- [2] K. Rubin, M. Sjoquist, A. Gustafsson, B. Isaksson, G. Salvessen and R. K. Reed, "Lowering of tumoral interstitial fluid pressure by prostaglandin E1 is paralleled by an increased uptake of Cr-EDTA," *Int. J. Cancer*, vol. 86, pp. 636-643, 2000.
- [3] P. A. Netti, D. A. Berk, M. A. Swartz, A. J. Grodzinsky and R. K. Jain, "Role of extracellular matrix assembly in interstitial transport in solid tumors," *Cancer Research*, vol. 60, pp. 2497-2503, 2000.
- [4] B. Han, E. Grassl, V. Barocas, J. Coad and J. C. Bischof, "A cryoinjury modeling using engineered tissue equivalents for cryosurgical applications," *Annals of Biomedical Engineering*, vol. 33, pp. 980-990, 2005.
- [5] B. Han, J. D. Miller and J. K. Jung, "Freezing-induced fluid-matrix interaction in poroelastic material," *Journal of Biomechanical Engineering*, vol. 131, pp. 021002, 2009.

- [6] S. Ikekawa, K. Ishihara, S. Tanaka and S. Ikeda, "Basic studies of cryochemotherapy in a murine tumor system," *Cryobiology*, vol. 22, pp. 477-483, 1985.
- [7] D. M. Clarke, J. M. Baust, R. G. Van Buskirk and J. G. Baust, "Chemo-cryo combination therapy: an adjunctive model for the treatment of prostate cancer," *Cryobiology*, vol. 42, pp. 274-285, 2001.
- [8] L. M. Mir and B. Rubinsky, "Treatment of cancer with cryochemotherapy," *British Journal of Cancer*, vol. 86, pp. 1658-1660, 2002.
- [9] A. A. Gage and J. G. Baust, "Cryosurgery for tumors - A clinical overview," *Technology in Cancer Research and Treatment*, vol. 3, pp. 187-199, 2004.
- [10] C. Nicholson and L. Tao, "Hindered diffusion of high molecular weight compounds in brain extracellular microenvironment measured with integrative optical imaging," *Biophysical Journal*, vol. 65, pp. 2277-2290, 1993.
- [11] R. G. Thorne and C. Nicholson, "In vivo diffusion analysis with quantum dots and dextrans predicts the width of brain extracellular space," *PNAS*, vol. 103, pp. 5567-5572, 2006.
- [12] C.-L. Wang, K. Y. Teo and B. Han, "An amino acidic adjuvant to augment cryoinjury of MCF-7 breast cancer cells," *Cryobiology*, vol. 57, pp. 52-59, 2008.
- [13] J. Sun, B. F. Lyles, K. H. Yu, J. Weddell, J. Pople, M. Hetzer, D. D. Kee and P. S. Russo, "Diffusion of dextran probes in a self-assembled fibrous gel composed of two-dimensional arborols," *Journal of Physical Chemistry B*, vol. 112, pp. 29-35, 2008.